

LASER INTERFEROMETER GRAVITATIONAL WAVE OBSERVATORY
- LIGO -
CALIFORNIA INSTITUTE OF TECHNOLOGY
MASSACHUSETTS INSTITUTE OF TECHNOLOGY

Technical Note	LIGO-T1500040-v1	2015/01/30
Homodyne Detector		
T. Isogai		

Distribution of this document:
LIGO Scientific Collaboration

California Institute of Technology
LIGO Project, MS 18-34
Pasadena, CA 91125
Phone (626) 395-2129
Fax (626) 304-9834
E-mail: info@ligo.caltech.edu

Massachusetts Institute of Technology
LIGO Project, Room NW22-295
Cambridge, MA 02139
Phone (617) 253-4824
Fax (617) 253-7014
E-mail: info@ligo.mit.edu

LIGO Hanford Observatory
Route 10, Mile Marker 2
Richland, WA 99352
Phone (509) 372-8106
Fax (509) 372-8137
E-mail: info@ligo.caltech.edu

LIGO Livingston Observatory
19100 LIGO Lane
Livingston, LA 70754
Phone (225) 686-3100
Fax (225) 686-7189
E-mail: info@ligo.caltech.edu

1 Motivation

Many quantum noise experiments use a balanced homodyne detector as a way to measure quantum noise. For example, the H1 squeezing experiment used a homodyne detector developed at AEI (AEI design: Ref.[1]) and successfully measured audio-band frequency squeezing. For the next generation low frequency squeezer, however, a few additional features for homodyne detector may become useful.

First, we would like to read out the individual photodiode (PD) signal besides the two PD difference signal. For one thing, this allows us to track the LO power (hence the shot noise level) as we take squeezing spectrum.

Second, we would like to reduce the possibility of malfunctioning components by minimizing the functionality on the homodyne electronics because we might place a homodyne detector in vacuum and we cannot replace any components once the circuit board was placed into a vacuum compatible enclosure (the box will be sealed completely by welding).

Third, we would like to use two different PDs (ETX500 from JDSU [2] and the high quantum efficiency InGaAs PDs from Laser Components [3]) with one circuit design.

Lastly, the AEI homodyne detector has only one RF resonance circuit, but we might want to have two RF resonance frequencies which may become useful for some fancy locking schemes.

The objective of this new homodyne detector is to incorporate the above features, while keeping it quite general so that it can accommodate to various quantum noise experiments.

2 Design

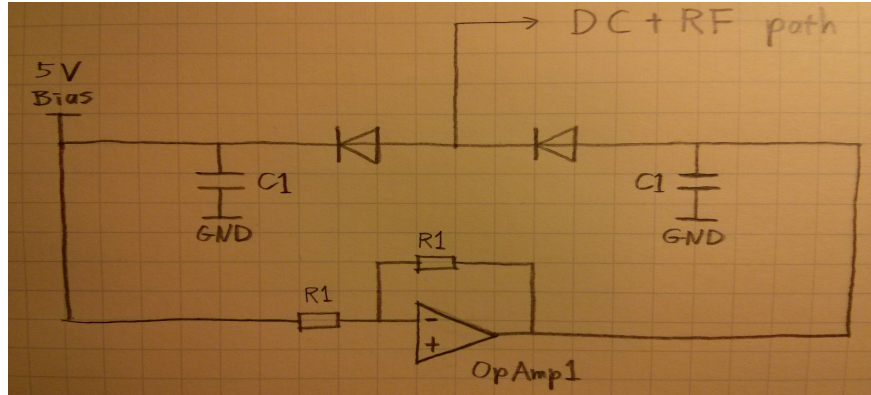
The actual schematic and PCB design can be found at [4]. There are four additional features compared to the conventional homodyne detector.

2.1 Individual PD Output

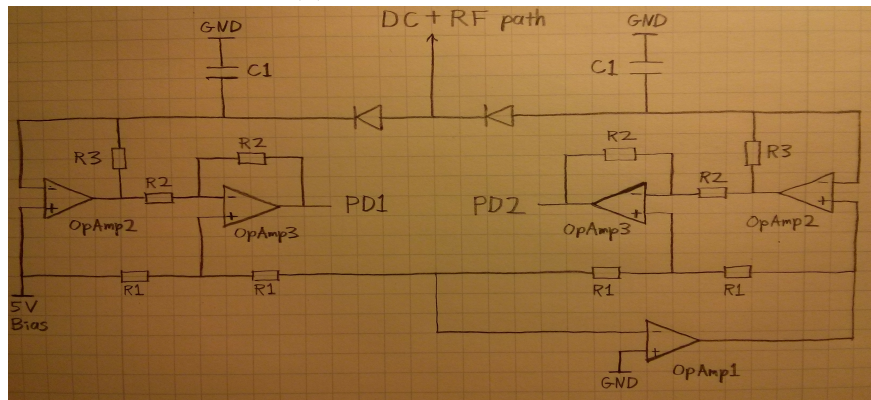
The basic idea to read out the individual PD signal is shown in Fig.1. The inverting OpAmp1 provides $-5V$, and the OpAmp2's keep the $\pm 5V$ reverse bias voltage for the PDs. When light hits the PD, the current produced by the PD goes through R3. Then OpAmp3 measures the voltage drop across R3. The OpAmp3's have an appropriate bias on the "+" input so that we get 0V when the PD is dark. The construction is symmetric around the DC/RF difference signal path, so that noises in the bias voltage are common to the both PDs and get rejected in the subtraction.

2.2 Vacuum Compatibility

Some experiments are going to place a homodyne detector (and an OPO) in vacuum to reduce the back scattering noise due to path length fluctuation. The circuit board size and the PDs' height are matched with that of the LSC/ASC RFPD board, so that we can re-use their vacuum enclosure design (Ref.[5]). Since it is difficult to replace any broken circuitry



(a) Conventional Design



(b) New Design

Figure 1: A simplified schematic that shows how the new design reads out the individual PD signal on top of the difference signal.

once we seal the circuit board in a vacuum enclosure, we need to minimize the possibility of broken components by putting away any functionality that can be done outside of vacuum.

On the other hand, since vacuum enclosures are expensive, some experiments are going to place a homodyne detector in air with a cheaper RF box, and may want to have a demodulator in one box for convenience.

To reconcile both needs, we decided to have the demodulation part of the circuit on a separate board, which can piggy-back ride on the main board. This way, we can take out the demodulation part of the board when we place a homodyne in vacuum, or we can put both the main and demodulation boards in one RF box if desired. Please see Ref.[4] for the demodulation board design, and Sec.5 for the vacuum enclosure design.

2.3 Compatibility with two different PD footprints

In the lab, we have been using two different types of PDs. One is from Laser Components (Ref.[3]); they have very high quantum efficiency, but are very expensive. The other is ETX500 from JDSU (Ref.[2]); they are less expensive and can be used when lower quantum efficiency ($\sim 90\%$) can be tolerated.

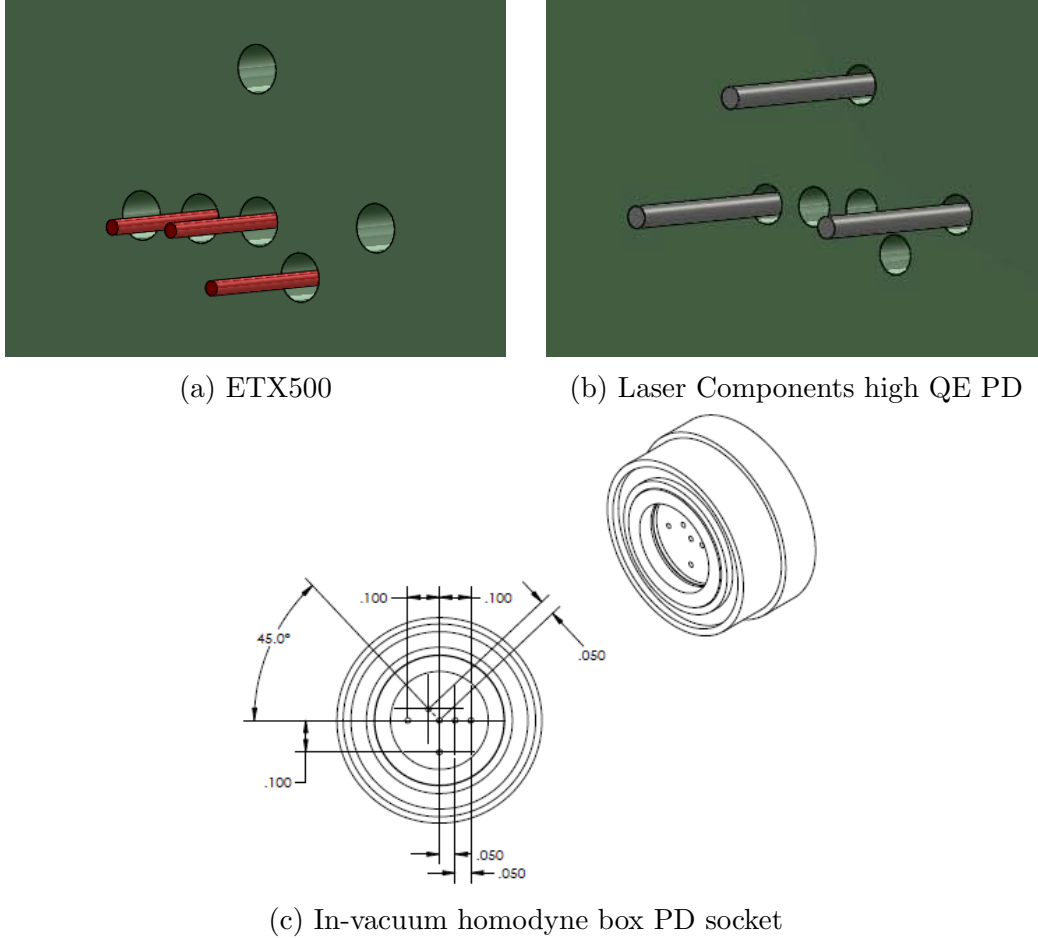


Figure 2: (a) and (b) show two different types of PD pins on the circuit board. (c) is the PD socket design for the in-vacuum homodyne enclosure.

They have different footprint (Ref.[6]), but it would be nice if one circuit board/enclosure design could handle both of them so that we can interchange two types of PDs (for example, we can use the inexpensive ones for proto-typing, and change to the high quantum efficiency PDs later). The new design of the circuit board and the vacuum enclosure supports both types of PD footprint (see Fig.2).

2.4 Two RF Resonant Circuits

The conventional design [1] has only one RF resonant circuit, which we use to lock the LO phase. For the next generation squeezing experiment, we might want to use two RF resonant circuits for some fancy locking schemes, and leaving the option of two demodulation frequencies ensures the flexibility. By tuning the resonant circuit (C40, C43 and L8 for the first resonance, and C49, C53 and L11 for the second resonance), the resonant frequencies can be changed as desired.

3 Response

3.1 DC response for difference signal

The difference signal between the two PDs is our main output where we measure quantum noise. The DC response for the difference signal is shown in Fig.3. This detector has roughly 800kHz bandwidth, which is usually high enough to detect audio band frequency squeezing (typically $< 100\text{kHz}$).

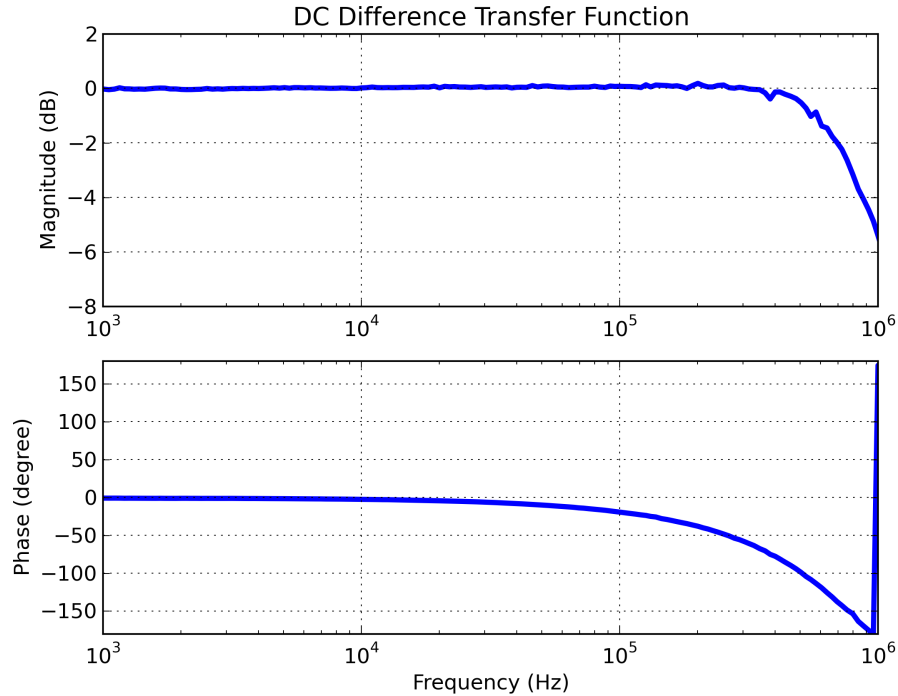


Figure 3: A transfer function of the DC difference signal path. The -3dB point is $\sim 800\text{kHz}$.

3.2 RF response

The RF resonant frequencies can be tuned (C40, C43 and L8 for the first resonance, and C49, C53 and L11 for the second resonance), and Fig.4 shows an example resonance at around 29.5MHz.

3.3 DC response for individual PD output

The individual PD outputs are meant to be diagnostic channels, and not designed as low noise or high bandwidth. A transfer function is shown in Fig.5. These outputs have about 300Hz bandwidth.

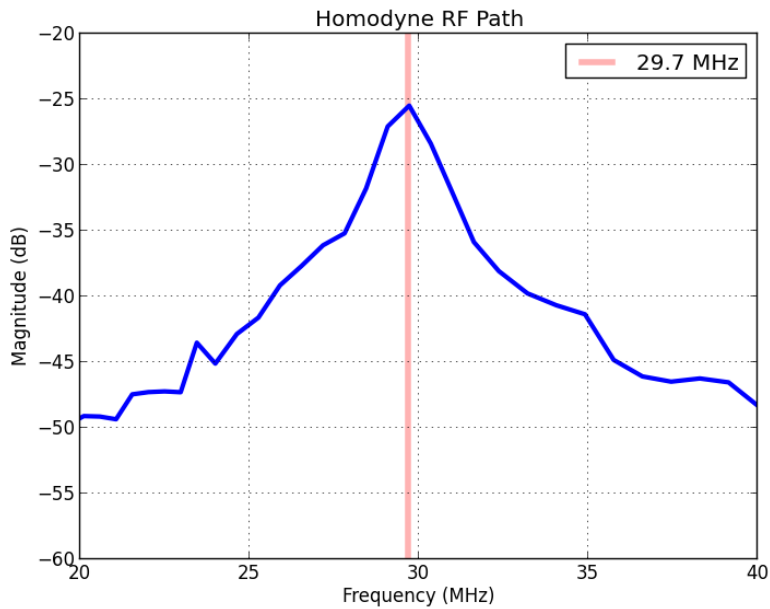


Figure 4: A transfer function of the RF resonance circuit. It is tuned to have a ~ 29.5 MHz resonance.

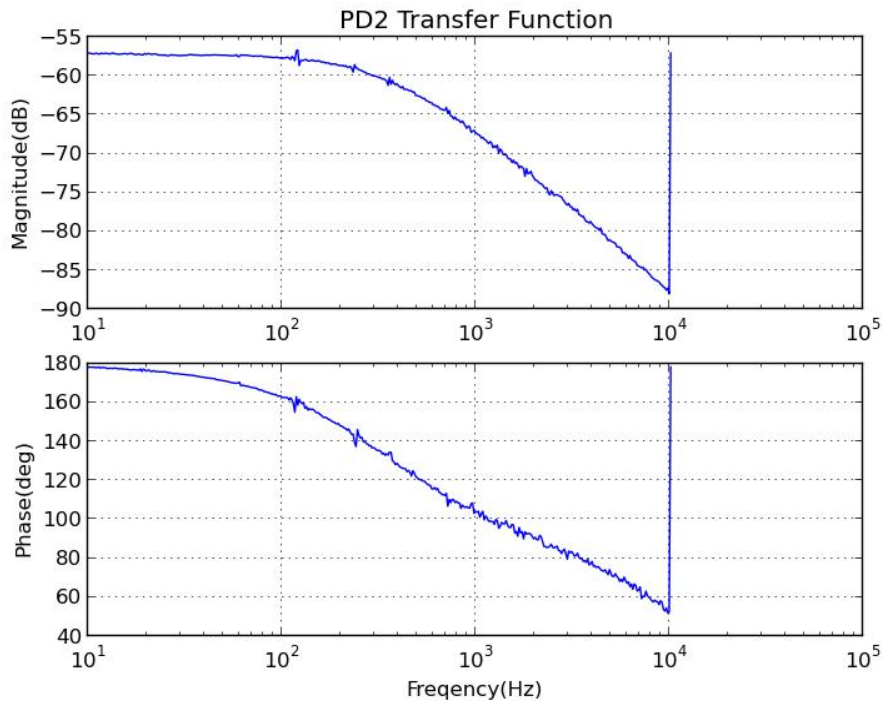


Figure 5: The individual PD output transfer function.

3.4 Demod Board

An optional demodulation board can be attached to the main circuit. This should be useful when you are using homodyne in air and want to demodulate the Rf signal in one box. A

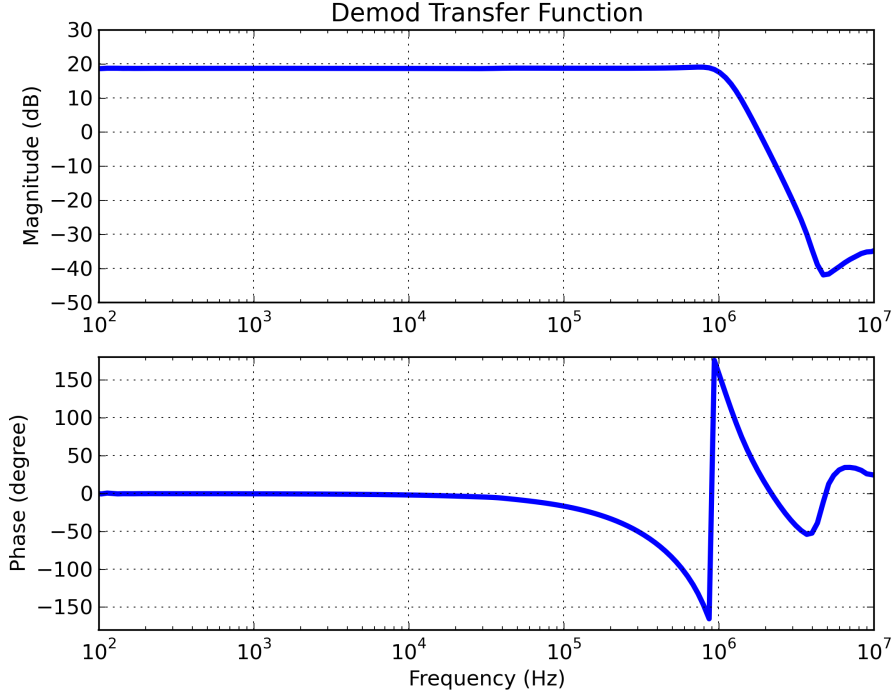


Figure 6: A transfer function of the demod board (the lowpass and gain stage after a mixer). It has a 4th order lowpass at around 1MHz with ~ 20 dB gain.

transfer function of this demodulation board (the lowpass and gain stage after a mixer) is shown in Fig.6.

4 Noise Performance

The homodyne detector has a transimpedance gain of 10k. From that 10k Ω resister, we expect the detector to have ~ 13 nVrms/ $\sqrt{\text{Hz}}$ electronics Johnson noise. For actual measurements, spectrum analyzers usually have some input noise. For example, Stanford Research Systems SR785 claims to have < 10 nVrms/ $\sqrt{\text{Hz}}$ input above 200Hz. So the upper bound for the Johnson noise measured by an SR785 is:

$$\sqrt{(13\text{nVrms}/\sqrt{\text{Hz}})^2 + (10\text{nVrms}/\sqrt{\text{Hz}})^2} = 16\text{nVrms}/\sqrt{\text{Hz}} \quad (1)$$

Therefore, we expect to measure $13 \sim 16$ nVrms/ $\sqrt{\text{Hz}}$ dark noise floor (valid above 200Hz) using an SR785. See Fig.7 for an actual measurement.

For a typical 1mW LO power, we expect (and measured) the shot noise to be at:

$$\text{ASD}(f) = R_\lambda \sqrt{2h\nu\bar{P}} \quad (2)$$

where $\bar{P} \sim 1\text{mW}$ is the averaged power of the LO field and R_λ (V/W) is the responsivity of

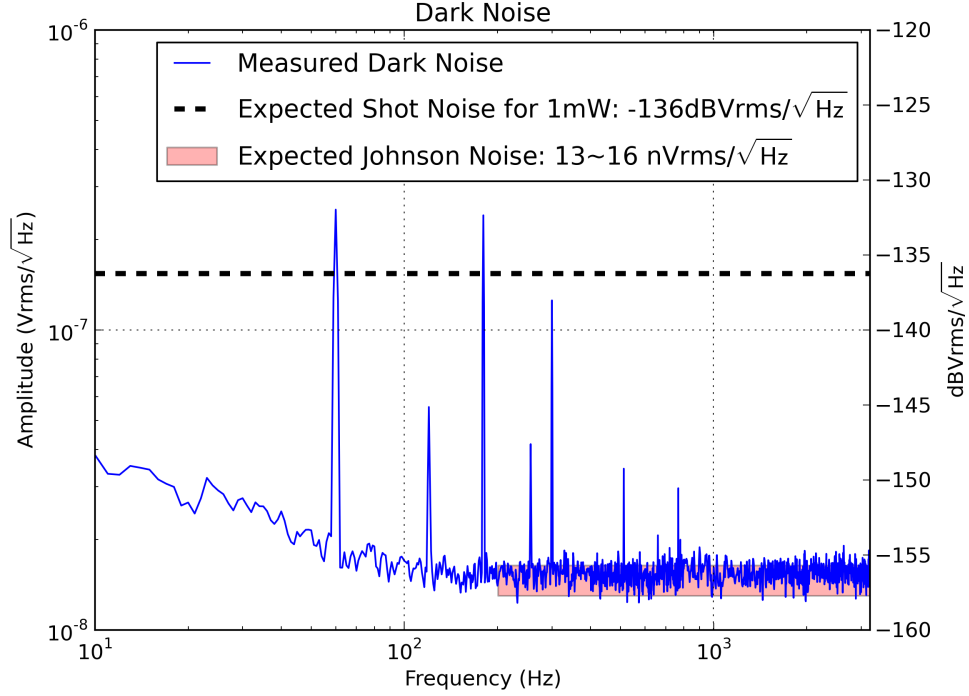


Figure 7: The expected $13 \sim 16 \text{ nVrms}/\sqrt{\text{Hz}}$ dark noise floor (valid above 200Hz) from the transimpedance resistor Johnson noise is shown in transparent red. This agrees well with the measurement. The 60Hz harmonics are pickups from a bad D-sub ribbon cable used at the time of measurement, and can be suppressed with an appropriate cable.

the homodyne detector:

$$\begin{aligned}
 R_\lambda &= \frac{\lambda e}{hc} \times \frac{\text{Quantum Efficiency}}{\text{Transimpedance Gain}} \\
 &= \frac{\lambda}{1240 \text{ W}\cdot\text{nm}/\text{V}} \times \frac{\text{Quantum Efficiency}}{\text{Transimpedance Gain}} \\
 &= \frac{1064 \text{ nm}}{1240 \text{ W}\cdot\text{nm}/\text{V}} \frac{93\%}{10\text{k}} \\
 &\sim 79.8 \text{ nV/mW}
 \end{aligned} \tag{3}$$

Thus, a one sided amplitude spectral density of the shot noise is $154 \text{ nVrms}/\sqrt{\text{Hz}}$ (or in dB unit, $-136 \text{ dBVrms}/\sqrt{\text{Hz}}$). We have roughly 20dB margin between the dark noise and a typical shot noise level (see Fig.7).

5 Enclosure

For in-vacuum homodyne enclosure, we intentionally made the circuit board size and the PDs' height the same as that of the LSC/ASC RFPD board, so that we can re-use their vacuum enclosure design (Ref.[5]). There are a few modifications, however.

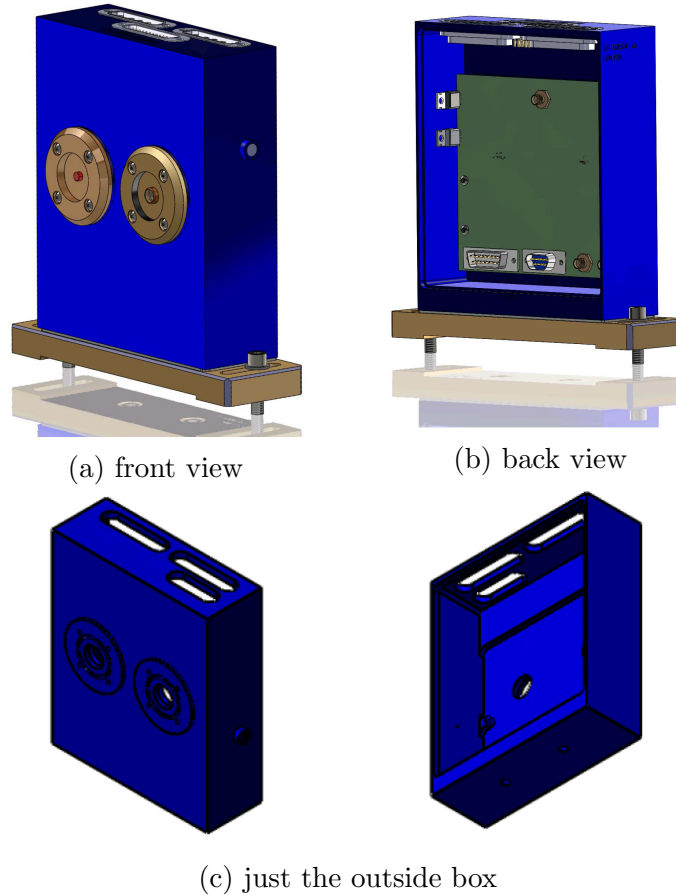


Figure 8: In-vacuum homodyne enclosure

First, the box layout was changed to have two PDs instead of one, and the PD footprint was also modified to be compatible with two different PD types (see Sec.2.3).

Second, the connector feedthroughs were modified to suit the homodyne circuit input/output. The homodyne in-vacuum enclosure has one 15-pin D-sub feedthrough, and two 5-pin SMP to coax feedthroughs. The latter is the same feedthrough as the one used for the ASC/LSC RFPD in-vacuum enclosure, so similar connectors can be used to bring the signals out of a vacuum chamber (Ref.[7]). All the DC output signals are both on the D-sub and SMP.

Lastly, the positions of the screw holes where the circuit board is supported is different from those of the ASC/LSC RFPD in-vacuum enclosure.

The complete design of the homodyne in-vacuum enclosure can be found in Ref.[8].

If you prefer not to use the in-vacuum enclosure, you can buy a much cheaper RF box and fit the circuit board inside it with some machining. For example, for the filter cavity experiment at MIT, we used a RF box 1590XX by Hammond Manufacturing (Ref.[9]).

References

- [1] Original AEI homodyne
http://emvogil-3.mit.edu/~isogait/Homodyne_Modified/Original/
- [2] ETX500 PD
http://emvogil-3.mit.edu/~isogait/Homodyne_Modified/Original/ETX500.pdf
- [3] Laser Components high quantum efficiency PD
http://emvogil-3.mit.edu/~isogait/Homodyne_Modified/Quotation_96129_08_04_2011.pdf
- [4] Homodyne circuit design:
<https://dcc.ligo.org/LIGO-D1300671>
- [5] LIGO DCC documents on the LSC/ASC RFPD vacuum enclosure
<https://dcc.ligo.org/LIGO-D1101992>
<https://dcc.ligo.org/LIGO-D1102003>
- [6] JDSU ETX500 footprint:
http://emvogil-3.mit.edu/~isogait/Homodyne_Modified/Original/ETX500.pdf
Laser Components high quantum efficiency PD footprint:
<http://www.jedec.org/sites/default/files/docs/archive/to/to-005.pdf>
http://emvogil-3.mit.edu/ilog/pub/ilog.cgi?group=lasti&date_to_view=09/05/2014&anchor_to_scroll_to=2014:09:05:20:52:10-eoelker
- [7] DCC documents about ASC/LSC RFPD in-vacuum enclosure feedthroughs and connectors:
<https://dcc.ligo.org/LIGO-D1101617>
<https://dcc.ligo.org/LIGO-D1300466>
<https://dcc.ligo.org/LIGO-D1300467>
<https://dcc.ligo.org/LIGO-D1101689>
- [8] Homodyne in-vacuum enclosure design:
<https://dcc.ligo.org/LIGO-D1400405>
- [9] In-air RF box; Hommond Manufacturing 1590XX:
<http://www.hammondmfg.com/pdf/1590XX.pdf>